metals

MDPI

Article

Corrosion Wear Performance of Pure Titanium Laser Texturing Surface by Nitrogen Ion Implantation

Lin Cao [1], Yun Chen [1], Jie Cui [2], Wei Li [1], Zhidan Lin [1,*] and Peng Zhang [1,*]

[1] Institute of Advanced Wear & Corrosion Resistant and Functional Materials, Jinan University, Guangzhou 510632, China; linc19993@163.com (L.C.); chenyun1518@126.com (Y.C.); liweijnu@126.com (W.L.)

[2] Analytical and Testing Center, South China University of Technology, Guangzhou 510640, China; czcuijie@scut.edu.cn

* Correspondence: linzd@jnu.edu.cn (Z.L.); tzhangpeng@jnu.edu.cn (P.Z.); Tel.: +86-020-8522-0890 (Z.L.); +86-020-8522-3562 (P.Z.)

Received: 19 June 2020; Accepted: 17 July 2020; Published: 22 July 2020

Abstract: The poor tribological performances of titanium have significantly limited its applications in the field of artificial joints. In order to solve problems regarding the wear and corrosion of artificial joints in the body, we fabricated the composite materials utilizing the combination of laser surface texturing and nitrogen ion implantation technology, and investigated the effect of laser surface texturing, nitrogen ion implantation, and different dimple area densities on tribological performance. The results show that the textured surface could reduce the friction coefficient and improve the wear resistance, and the optimum dimple density was found to be 25%. After N ion implantation, the wear resistance of the textured sample was further improved, due to the formation of the nitride layer. Moreover, as shown by the electrochemical test results, the corrosion resistance was enhanced significantly. The friction coefficient decreased the most, and the wear resistance increased by 405% with the lowest wear rate of 0.37×10^{-3} mm^3/N·m. However, the specimen with a dimple density of 60% had the worst wear resistance. The results of the study provide a basis for the development and application of artificial joint materials.

Keywords: laser surface texturing; nitrogen ion implantation; wear and corrosion; electrochemical

1. Introduction

The demand for titanium implants has grown extensively in previous years. This has been driven by an ageing population and the desire for hard tissue repair [1–3]. However, the poor tribological properties of pure titanium, including a high friction coefficient, severe adhesive wear, and sensitivity to fretting wear strongly restrict its application. Particular attention should be given to the wear and corrosion products that can lead to a reduction in osseointegration [4] and induce tissue inflammation in the human body [5], which would form for the poor wear properties of titanium. In order to resolve the tribological problems of titanium, various surface modification technologies have been proposed. Surface texturing, in which an artificial topography fabricated on the surface enhances titanium tribological properties, is one of the most promising approaches. Numerous studies have shown that surfaces with patterns at the micro scale, such as dimples [6], lines [7], or nets [8], have better anti-friction and wear resistance performance than flat and smooth surfaces. A comprehensive study on its anti-wear and friction mechanisms was also reported recently. This unsmooth surface structure decreases the real contact area and wear debris entrapment and causes a local increase in the lubricant supply by fluid reservoirs, as well as an increase in load-carrying capacity through a hydrodynamic effect [9]. So, the unsmooth texture surface can have better wear resistance under some conditions.

Roy's study [10] showed that a dimpled surface with a 400 μm dimple diameter is associated with a significant improvement in tribological performance, including reductions of nearly 22% for friction and 53% for wear. In order to obtain this textured surface, several surface texturing techniques have been adopted. Compared to other surface texturing techniques, such as mechanical machining [11,12], ion beam texturing [13], and chemical etching [14], laser surface texturing (LST) [15–20] possesses more versatility, faster adaptability, higher precision, and a cleaner environment. This technique was applied to prepare the micrometer-sized features presented in this paper. Many studies have been conducted on the laser textured surface with dimple geometry. Hu et al. [18] produced dimple textures with different diameters on Ti-6Al-4V surfaces and observed that the dimple pattern leads to a lower friction coefficient and wear, compared with an untextured surface under oil lubrication conditions. Moreover, LST has been found to be capable of effectively increasing the critical load of the substrate [19] and prolonging the wear life of the textured surface when combined with a lubricant [20]. Although surface texturing could enhance the frictional properties of titanium-based materials, the mechanical strength of the materials needs to be further improved to meet the requirements of practical application.

However, LST does not significantly improve the mechanical properties of the treated specimen surface. Titanium nitride coating is the best choice for solving this problem. On the one hand, titanium nitride (TiN) is widely used as a coating material due to its high hardness, wear resistance, and corrosion inertness in biological solutions [21,22]. On the other hand, the TiN/Ti_2N-containing layer provides new possibilities for producing a non-toxic, biocompatible surface layer on titanium and its alloys [23]. Various techniques have been employed for the synthesis of TiN [24–27]. Among these, nitrogen ion implantation (NII) is also a promising alternative for improving and functionalizing the surfaces [28].

Though both of these treatments have been shown to improve the relative performance of the base material, there has been little research on the combination of the two techniques reported in recent years. So, this study focuses on the effect of the combination of LST and NII treatments on the wear and corrosion resistance of pure titanium surfaces in modified-simulated body fluid (m-SBF). Among them, samples with three different dimple area densities are prepared, to investigate how the texture density affects the corrosion-wear performance.

2. Materials and Methods

2.1. Preparation (LST and NII Treatment)

Commercially available pure titanium (purchased from the Northwest Non-ferrous Institute of Technology in Xi'an, China) selected as the test substrate materials were cut to specimens with a dimension of 2 mm × 10 mm × 15 mm. As prepared specimens were ground using silica papers of 400, 600, 800, 1200, and 1500 grit, in turn, and cleaned ultrasonically in ethyl alcohol, and then mechanically polished up to a surface roughness of about 0.1 μm.

LST was carried out using a pulsed Nd:YAG laser (produced by Chutian Laser Group Co. Ltd., Wuhan, China), with a wavelength of 1064 nm and a pulse width of 0.25 ms, to obtain textured surface with different dimple density in argon atmosphere. The parameters of the laser textured surface are shown in Table 1. For removing the bulges or burrs around the rim of the dimples, it is indispensable to experience a mild re-polishing after the laser texturing treatment and ultrasonic re-cleaning in ethyl alcohol. Ion implantation equipment was used for nitrogen ion implantation (NII) treatment for the textured specimens by a Kaufman gas ion source (Southwestern Institute of Physics, Chengdu, China). Prior to implantation, the initial gas pressure in the implantation chamber was under 3×10^{-3} Pa. Nitrogen was implanted into the above the textured titanium to produce TiN layer modified samples with implantation doses of 1×10^{18} ions/cm^2.

Table 1. Characteristics of the laser-textured dimple patterns. (tx: textured and implanted samples with a dimple density).

Specimen	Diameter (μm)	Pitch (μm)	Dimple Density
CP Ti	-	-	-
tx 25%	400	700	25%
tx 35%	400	600	35%
tx 60%	400	450	60%

2.2. *Surface Characterization*

The structural properties of these thin films were studied by Grazing incidence small-angle X-ray scattering (GISAXS) (XRD, Rigaku MiniFlex600, Japanese Science, Tokyo, Japan). The Grazing incidence is 3°. The diffraction angle ranged from 20° to 80°, and a scanning rate of 4°/min was used. The surface microstructure and cross-section morphologies of the samples were observed by scanning electron microscopy (SEM, Phenom XL, Delft, Holland). The roughness was measured by the contact profile scanner. Digital Micro Hardness Tester (HXD-1000TMSC/LCD, Shanghai Caikang Optical Instrument Factory, Shanghai, China) was used to measure the microhardness of the treated specimens.

2.3. *Electrochemical and Tribocorrosion Tests*

The corrosion behavior of TiN coatings in the m-SBF solution (Table S1 [29]) was investigated electrochemically. A standard three electrode corrosion cell (the specimen as the working, a saturated calomel electrode (SCE) as the reference and high purity platinum as the counter electrode) was used. Tafel curves were recorded at a potential range from −0.25 to +0.25 mV, and a scanning rate of 1 mV/s. Each test was repeated three times to ensure reproducibility. The electrochemical impedance spectroscopy (EIS) was performed on the flexible electrode using a Princeton PARSTAT 4000 electrochemical station. The scanning frequencies ranged from 10^5 to 10^{-2} Hz, and the amplitude was of about 20 mV.

Tribological tests were conducted using a reciprocating sliding tribometer (MFT-R4000, Lanzhou Institute of Chemical Physics, Chinese Academy of Science, Lanzhou, China) in the ball-on-disc mode with the stroke length of 5 mm, applied load of 5 N, sliding frequency of 0.2 Hz. The average wear volume was measured by a 3D surface morphology analyzer (BMT EXPERT, Lanzhou Huahui Instrument Technology CO., Ltd, Lanzhou, China). The upper specimen was an φ6 mm Al_2O_3 ball, and the bottom is the textured sample. Prior to the test in m-SBF solution for 60 min at room temperature, the open circuit potential (OCP) was recorded for 15 min and, after the sliding, continued for 15 min. Every test was carried out at least three times with completely new pellets, and the worn surfaces investigated using SEM. After Tribological tests, the wear rate was calculated by the following equation:

$$W = \frac{\Delta V}{S \cdot F} = \frac{A \cdot D}{2D \cdot f \cdot t \cdot F} = \frac{A}{2 f \cdot t \cdot F} \times 10^3 \quad (1)$$

where A is the wear scar cross-sectional area, mm^2; D is the glide amplitude during the wear test, mm; f is the frequency of the reciprocating wear process, Hz; t is the glide time during the wear test, s.

3. Results and Discussion

Figure 1a–c show the surface morphologies of the titanium with LST treatment, where three dimple area densities of 25%, 35%, and 60% were achieved. Here, the dimple area density is defined as the ratio of the dimple area to the entire area. Due to the high energy density of the laser irradiation, the instantaneous high temperature of tens of thousands of degrees centigrade formed near the laser spot on the surface of TA2, so the material at the focal point position instantaneously melted or vaporized, and a molten pool pit bottom with many ripples appeared. Figure 1d shows the SEM images of the cross section of the sample after LST treatment. The depth of the sample pits was approximately 170 μm.

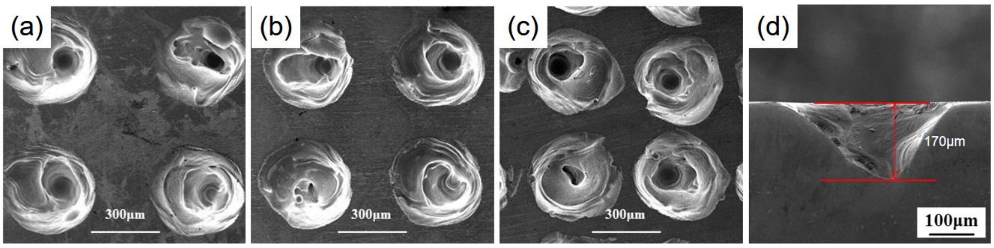

Figure 1. Scanning electron microscopy (SEM) images of laser textured surfaces corresponding to dimple patterns with dimple area densities of (**a**) 25%, (**b**) 35%, and (**c**) 60%; (**d**) SEM images of the cross section of the textured dimple.

Figure 2a shows the XRD patterns of the titanium samples that underwent laser surface texturing (LST) treatment and nitrogen ion implantation (NII) treatment, and no treatment, respectively. As can be seen from Figure 2b, there was no significant difference in the compositions of the textured and untreated samples, and a unique set of diffraction peaks of the α-Ti phase appeared, indicating that no titanium oxide formed on the surface of the specimens with the laser texturing process in an argon atmosphere. In comparison with the textured samples, TiN (face centered cubic JCPDS file No. 38-1420) and Ti_2N (tetragonal JCPDS file No. 23-1455) phases were formed on the surface of the specimens with NII treatment and made it bright yellow, as shown in Figure 2a. The thickness of the titanium nitride layers on the surface of the pure titanium with NII treatment was measured to be approximately 1 μm, as shown in Figure 2c. The NII film layer was uniform.

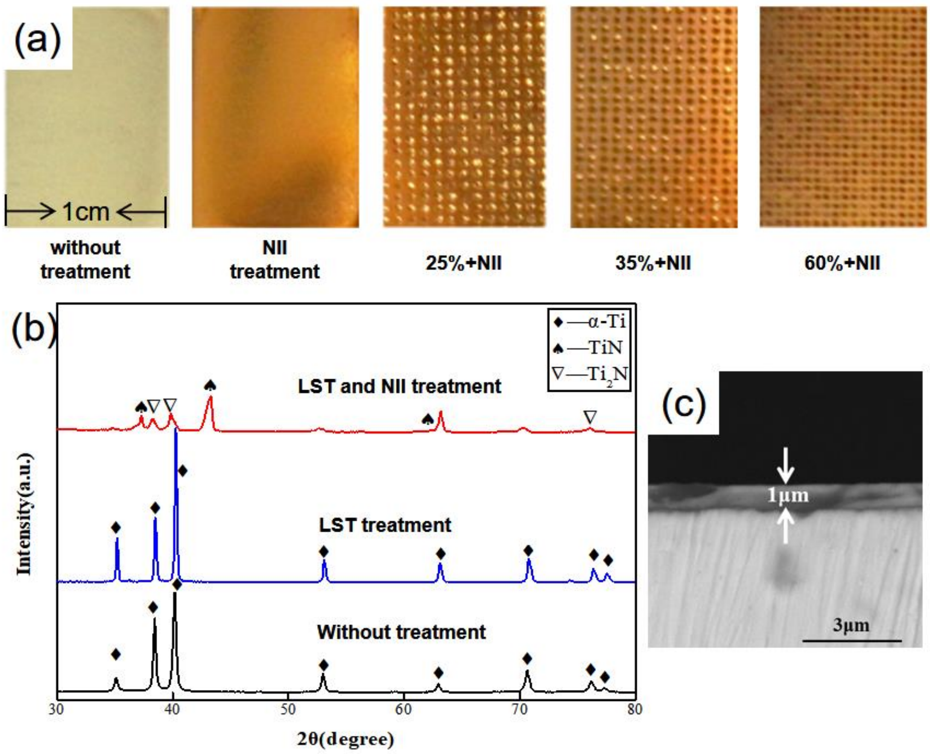

Figure 2. (**a**) Photographs of textured specimens with nitrogen ion implantation (NII) treatment; (**b**) X-ray diffraction patterns of Table 2. with laser surface texturing (LST) and NII treatment; (**c**) SEM image of the cross-section of the pure titanium with NII treatment.

Table 2. Values of EIS resistances of the textured samples with NII treatment in m-SBF solution.

Sample Name	CP Ti	N + CP Ti	N + tx 25%	N + tx 35%	N + tx 60%
R_s (Ω/cm^2)	24.63 ± 2.57	28.31 ± 1.98	42.16 ± 1.85	30.97 ± 2.94	21.9 ± 2.01
R_a (Ω/cm^2)	-	127.90±8.41	422.50 ± 19.15	383.2 ± 5.87	188.4 ± 24.19
R_b ($k\Omega/cm^2$)	405.7 ± 10.08	1393.5±60.66	975.4 ± 57.24	860.4 ± 45.92	847.4 ± 45.36

As shown in Figure 3, the frictional coefficient of the samples decreased to varying degrees after laser surface texturing. This means that the surface texture effectively reduced the coefficient of friction, and, when a TiN coating was generated on the surface, a large decrease was found in the sample with a dimple density of 25% after the nitrogen ion implantation process.

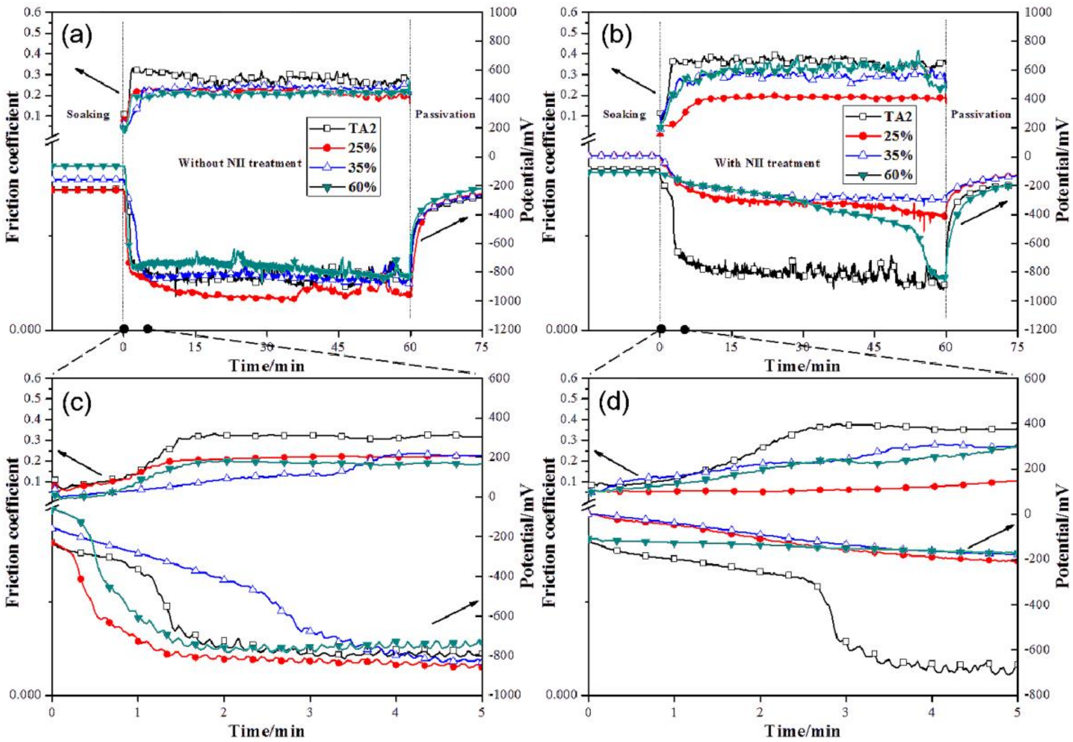

Figure 3. Friction coefficient of pure titanium in modified-simulated body fluid (m-SBF) solution at different dimple area densities and the typical tribo-corrosion curve with open circuit potential (OCP) values and the partially enlarged view (**a**) without NII treatment and the part of (**c**); (**b**) with NII treatment and the part of (**d**).

The tribo-corrosion process of the samples was composed of three main stages: soaking, sliding, and passivation. Passive films were produced after 15 min of soaking. The magnified view of the beginning of the sliding (the first 5 min) presented a symmetric relationship between the frictional coefficient and the OCP, indicating that the surface of the passive films was worn away with the onset of friction. Compared with the samples that underwent NII treatment, the passive films of the textured TA2 samples that did not undergo NII treatment were destroyed quickly, as soon as sliding began. This resulted in the OCP value dropping rapidly to approximately −800 mV, as shown in Figure 3a,b. On the contrary, the OCP values of the samples that underwent NII treatment decreased slowly, because the TiN coating limited the extent of damage caused by sliding, while the sample with a dimple density of 60% began to decrease dramatically after 55 min. This may be due to the fact that, as the dimple density increases, the edge of the dimples on the surface undergoes more cutting and ploughing per unit length, resulting in serious wear. All samples experienced different degrees of passivation after sliding.

Figure 4 shows SEM images of the worn surfaces of unimplanted and implanted samples with different dimple area densities for the wear test in m-SBF solution. The appearance of furrows in the SEM images shows that the main wear mechanism in the wear process is abrasive wear. Compared with TA2 (Figure 4a), the wear scar on the surface of each textured sample (Figure 4b–d) was relatively shallow, and the number of the furrows reduced, because the surface dimples helped to entrap wear debris during the sliding process. Compared with the samples without NII treatment, the nitrided samples showed narrower scratches. Obviously, the sample with a dimple density of 25% (Figure 4b) exhibited the narrowest wear scar. With an increase in the dimple density, the width and depth of the wear scar gradually increased. The implanted sample with a dimple density of 25% exhibited the narrowest and shallower wear scars. This shows that the surface texturing could help to improve the tribological properties to some extent.

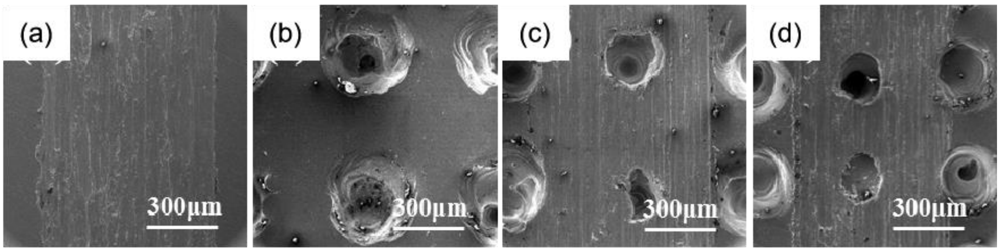

Figure 4. SEM images of the wear tracks for untextured (**a**) and textured specimens with a dimple density of 25%, (**b**), 35% (**c**), and 60% (**d**), with NII treatment in m-SBF solution.

The respective 2D and 3D profiles of the wear scar for the textured and implanted titanium samples characterized by the 3D surface morphology analyzer are displayed in Figure 5. Figure 5a shows some wear marks for the samples without LST treatment. However, compared with the samples without LST treatment, the wear track width and depth of the textured samples with NII treatment increased as the dimple density increased. It is notable that the sample with a dimple density of 25% (Figure 5c) had a narrow and shallow wear scar, showing good wear resistance. This can be traced back to the fact that, as the dimple density increases, the cutting between the Al_2O_3 ball and the edge of the dimples becomes more frequent during the rubbing, accelerating the wear of the surface.

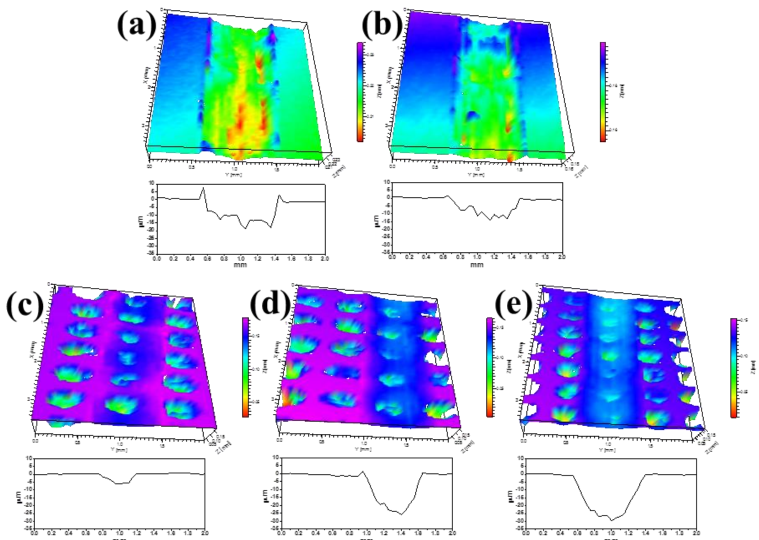

Figure 5. Three-dimensional profiles and section morphology of the resulting wear tracks of the sample without treatment (TA2) samples under different treatments in m-SBF solution: (**a**) TA2, (**b**) NII, (**c**) 25% LST + NII, (**d**) 35% LST + NII, (**e**) 60% LST + NII.

As can be seen from Figure 6, the hardness value of the textured sample increased compared with that of the untreated TA2 sample, which indicates that the heat affected zone that formed around the impact point of laser beam caused a certain strengthening on the surface of TA2. As the dimple density increased, the hardness of the textured samples increased. It was higher after NII treatment, due to the formation of hard titanium nitride. The wear rate of samples with LST and NII treatment was reduced, compared with that of the samples with LST treatment. This means that the titanium nitride coating helped to improve the wear resistance of the material. The wear rates of the textured and implanted samples with a dimple density of 25% (tx 25%) showed the lowest wear rates (about 0.37×10^{-3} mm^3/N·m), and the corresponding wear resistance increased by 405%, compared with 1.94×10^{-3} mm^3/N·m for the sample without treatment (TA2). However, the specimen with a dimple density of 60% had the worst wear resistance, which indicated was not higher the dimple density, its wear resistance, better.

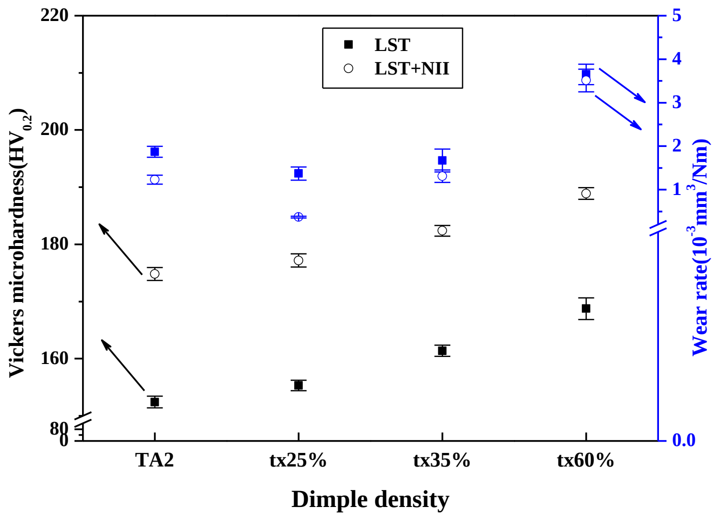

Figure 6. Wear rates and microhardness of textured TA2 samples after nitrogen ion implanting.

The impedance diagram, which was obtained from the Nyquist plots of the textured and implanted samples, is shown Figure 7, and its equivalent circuit diagram consisting of two constant phase elements (CPE) in parallel and three resistances, R_s, R_a, and R_b (related to the solution resistance, the resistance of the outer TiN layer, and the resistance of the middle compact layer, respectively) [30]. Compared with the TA2 samples, the implanted samples had higher total impedance values (R_s, R_a, and R_b, which were fitted by ZSimpWin software (Version, EChem Software, Ann Arbor, MI, USA), as shown in Table 2), which indicates that the surface had a larger corrosion resistance. The impedance of the compact passive inner layer of the implanted samples increased in comparison with that of the TA2 samples, which revealed, to a large extent, that the corrosion resistance of the sample could be improved by nitrogen ion implantation. Considering the textured samples, the implanted sample with a dimple density of 25% achieved the highest total impedance value of 975.8 kΩ/cm^2.

Figure 8 shows the potentiodynamic polarization curves of the textured samples after nitrogen implantation in m-SBF solution, and the corresponding corrosion parameters are shown in Table 3. The corrosion potential and corrosion current density of the titanium without treatment were 464.899 mV and 351.192 nA/cm^2, respectively. Obviously, the curves of all of the implanted samples moved to the right. For the corrosion current, it can be seen that the corrosion resistance of the nitrogen-injected samples was one order of magnitude higher than that of non-nitrogen-injected ones. With an increase in the textured area coverage, the corrosion current density of implanted samples increased successively and was lower than that of TA2, which could be because the part of the surface with irregular dimples that was not implanted with nitrogen also gradually increased. An improvement in corrosion resistance of the implanted samples in the m-SBF solution was achieved, which indicated that the TiN coatings help to reduce the tendency to corrode.

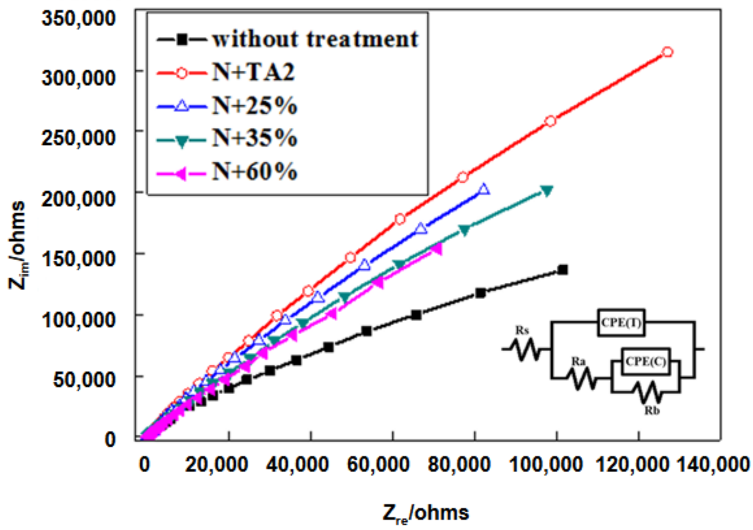

Figure 7. (**a**) Nyquist diagram of the textured samples after nitrogen implantation, (**b**) equivalent circuit diagram corresponding to electrochemical impedance spectroscopy (EIS) spectra, (**c**) schematic representation of the implanted titanium after laser surface texturing.

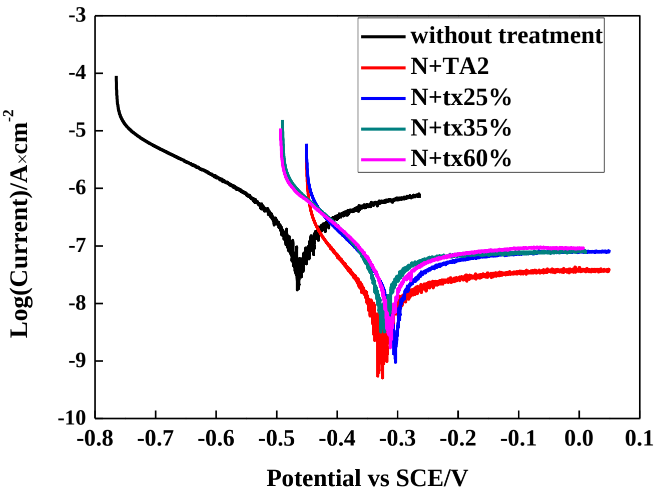

Figure 8. Potentiodynamic polarization curves of the textured samples after the addition of nitrogen.

Table 3. Corrosion current density and corrosion potential of the textured samples after nitrogen implantation in m-SBF solution.

Sample Name	CP Ti	N + CP Ti	N + tx 25%	N + tx 35%	N + tx 60%
E_{corr} (mV)	−464.899	−321.338	−298.476	−324.622	−305.288
I_{corr} (nA/cm^2)	351.192	11.833	23.993	30.936	22.407

4. Conclusions

In this study, industrial pure titanium was used as a matrix to fabricate the surface with different dimple area densities by a pulsed Nd:YAG laser. Then, nitrogen implantation was carried out on the textured surface for the purpose of creating a titanium nitride layer by NII. The wear and corrosion resistance of the as-fabricated samples were tested. The main conclusions from this study are summarized as follows: LST helped to improve the friction resistance of the material surface and the textured samples had lower friction coefficients. Compared to the samples without treatment, the wear resistance of the textured sample improved when m-SBF solution was used. Nitrogen ion implantation (NII) helped to further reduce the friction coefficient and improve the wear performance of the material surface, and, meanwhile, the corrosion resistance was enhanced by the presence of TiN coatings. The textured samples with a dimple density of 25% had the lowest wear rate of about 0.37×10^{-3} $mm^3/N \cdot m$, which was a considerably enhancement, compared with the sample without treatment (TA2), which had a wear rate of 1.94×10^{-3} $mm^3/N \cdot m$. The textured samples with a dimple density of 25% also had the highest total impedance value and a lower corrosion current density, which indicated better corrosion resistance.

Supplementary Materials: The following are available online at http://www.mdpi.com/2075-4701/10/8/990/s1, Table S1.

Author Contributions: Conceptualization, L.C., and Y.C.; methodology, P.Z.; software, Y.C.; validation, L.C. and Y.C.; formal analysis, L.C. and Y.C.; investigation, L.C. and Y.C.; resources, J.C., P.Z., Z.L. and W.L.; data curation, L.C.; writing—original draft preparation, L.C. and Y.C.; writing—review and editing, P.Z; supervision, P.Z.; project administration, P.Z.; funding acquisition, P.Z. and Z.L. All authors have read and agreed to the published version of the manuscript.

Funding: This research was funded by National Natural Science Foundation of China (51801065), Science and Technology Project of Guangdong Province (2015A030310488, 2014B090915003 and 2015B090901052) and the Scientific Cultivation and Innovation Fund Project of Jinan University (21617427).

Acknowledgments: National Natural Science Foundation of China (51801065), Science and Technology Project of Guangdong Province (2015A030310488, 2014B090915003 and 2015B090901052) and the Scientific Cultivation and Innovation Fund Project of Jinan University (21617427).

Conflicts of Interest: The authors declare no conflict of interest.

References

1. Banerjeea, D. Perspectives on Titanium Science and Technology. *Acta Mater.* **2013**, *61*, 844–879. [CrossRef]
2. Rack, H.J.; Qazi, J.I. Titanium Alloys for Biomedical Applications. *Mater. Sci. Eng. C* **2006**, *26*, 1269–1277. [CrossRef]
3. Jung, H.D.; Jang, T.S.; Wang, L.; Kim, H.E.; Koh, Y.H.; Song, J. Progress in Res. on the Surface/Interface of Materials for Hard issue Implant. *Biomaterials* **2015**, *37*, 49–61. [CrossRef] [PubMed]
4. Gu, Y.; Wang, Z.; Shi, J.; Wang, L.; Hou, Z.; Guo, X.; Tao, Y.; Wu, X.; Zhou, W.; Liu, Y.; et al. Titanium particle-induced osteogenic inhibition and bone destruction are mediated by the GSK-3β/β-catenin signal pathway. *Cell Death Dis.* **2017**, *8*, e2878. [CrossRef]
5. Lee, H.G.; Hsu, A.; Goto, H.; Nizami, S.; Lee, J.H.; Cadet, E.R.; Tang, P.; Shaji, R.; Chandhanayinyong, C.; Kweon, S.H.; et al. Aggravation of inflammatory response by costimulation with titanium particles and mechanical perturbations in osteoblast- and macrophage-like cells. *Am. J. Physiol. Cell Physiol.* **2013**, *304*, 431–439. [CrossRef]
6. Xiong, D.; Qin, Y.; Li, J.; Wan, Y.; Tyagi, R. Tribological properties of PTFE/laser surface textured stainless steel under starved oil lubrication. *Tribol. Int.* **2015**, *82*, 305–310. [CrossRef]
7. Vlădescu, S.C.; Olver, A.V.; Pegg, I.G.; Reddyhoff, T. Combined friction and wear reduction in a reciprocating contact through laser surface texturing. *Wear* **2016**, *358–359*, 51–61.
8. Zupančič, M.; Može, M.; Gregorčič, P.; Golobič, I. Nanosecond laser texturing of uniformly and non-uniformly wettable micro structured metal surfaces for enhanced boiling heat transfer. *Appl. Surf. Sci.* **2016**, *399*, 480. [CrossRef]
9. He, D.; Zheng, S.; Pu, J.; Zhang, G.; Hu, L. Improving tribological properties of titanium alloys by combining laser surface texturing and diamond-like carbon film. *Tribol. Int.* **2015**, *82*, 20–27. [CrossRef]
10. Roy, T.; Choudhury, D.; Ghosh, S.; Mamat, A.B.; Pingguan-Murphy, B. Improved friction and wear performance of micro dimpled ceramic-on-ceramic interface for hip joint arthroplasty. *Ceram. Int.* **2015**, *41*, 681–690. [CrossRef]
11. Qu, N.S.; Zhang, T.; Chen, X.L. Surface Texturing of Polyimide Composite by Micro-Ultrasonic Machining. *J. Mater. Eng. Perform.* **2018**, *27*, 1369–1377. [CrossRef]

12. Su, X.; Shi, L.; Huang, W.; Wang, X. A multi-phase micro-abrasive jet machining technique for the surface texturing of mechanical seals. *Int. J. Adv. Manuf. Technol.* **2016**, *86*, 1–8. [CrossRef]
13. Wang, X.; Kato, K. Improving the Anti-seizure Ability of SiC Seal in Water with RIE Texturing. *Tribol. Lett.* **2003**, *14*, 275–280. [CrossRef]
14. Ou, J.; Hu, W.; Liu, S.; Xue, M.; Wang, F.; Li, W. Superoleophobic textured copper surfaces fabricated by chemical etching/oxidation and surface fluorination. *Acs Appl. Mater. Interfaces* **2013**, *5*, 10035–10041. [CrossRef] [PubMed]
15. Kibria, G.; Sen, A.; Aziz, H.M.T.; Doloi, B.; Bhattacharyya, B. Pulsed Nd:YAG Laser Surface Texturing of Pure Titanium Material. In *Precision Product-Process Design and Optimization*; Springer: Singapore, 2018.
16. Etsion, I. State of the Art in Laser Surface Texturing. *J. Tribol.* **2005**, *127*, 761–762. [CrossRef]
17. Vilhena, L.M.; Sedlaček, M.; Podgornik, B.; Vižintin, J.; Babnik, A.; Možina, J. Surface texturing by pulsed Nd:YAG laser. *Tribol. Int.* **2009**, *42*, 1496–1504. [CrossRef]
18. Hu, T.; Hu, L.; Ding, Q. The effect of laser surface texturing on the tribological behavior of Ti-6Al-4V. *Proc. Inst. Mech. Eng. Part J J. Eng. Tribol.* **2012**, *226*, 854–863. [CrossRef]
19. Lin, N.; Li, D.; Zou, J.; Xie, R.; Wang, Z.; Tang, B. Surface Texture-Based Surface Treatments on Ti6Al4V Titanium Alloys for Tribological and Biological Applications: A Mini Review. *Materials* **2018**, *11*, 487. [CrossRef]
20. Rapoport, L.; Moshkovich, A.; Perfilyev, V.; Lapsker, I.; Halperin, G.; Itovich, Y.; Etsion, I. Friction and wear of MoS 2, films on laser textured steel surfaces. *Surf. Coat. Technol.* **2008**, *202*, 3332–3340. [CrossRef]
21. Ion, R.; Vasilescu, C.; Drob, P.; Vasilescu, E.; Cimpean, A.; Drob, S.I.; Gordin, D.-M.; Gloriant, T. Long-term corrosion performances and cytocompatibility of nitrided Ti and Ti–6Al–4V alloy in severe functional conditions. *Mater. Corros.* **2014**, *65*, 593–604. [CrossRef]
22. Rosca, J.C.M.; Vasilescu, E.; Drob, P.; Vasilescu, C.; Drob, S.I. Corrosion behaviour in physiological fluids of surface films formed on titanium alloys. *Mater. Corros.* **2015**, *63*, 527–533. [CrossRef]
23. Huang, H.H.; Hsu, C.H.; Pan, S.J.; He, J.L.; Chen, C.C.; Lee, T.L. Corrosion and cell adhesion behavior of TiN-coated and ion-nitrided titanium for dental applications. *Appl. Surf. Sci.* **2005**, *244*, 252–256. [CrossRef]
24. Ohtsu, N.; Saito, W.; Yamane, M. Thickness of titanium nitride layers formed by focused low-power pulsed Nd:YAG laser irradiation in nitrogen atmospheres. *Surf. Coat. Technol.* **2014**, *244*, 57–62. [CrossRef]
25. Tacikowski, M.; Morgiel, J.; Banaszek, M.; Cymerman, K. Structure and properties of diffusive titanium nitride layers produced by hybrid method on AZ91D magnesium alloy. *Trans. Nonferrous Met. Soc. China* **2014**, *24*, 2767–2775. [CrossRef]
26. Yazdani, A.; Soltanieh, M.; Aghajani, H.; Rastegari, S. A new method for deposition of nano sized titanium nitride on steels. *Vacuum* **2011**, *86*, 131–139. [CrossRef]
27. Secondo, R.; Avrutin, V.; Özgür, Ü.; Kinsey, N. Optimization of Titanium Nitride Films using Plasma Enhanced Atomic Layer Deposition. In Proceedings of the CLEO: Applications and Technology, San Jose, CA, USA, 13–18 May 2018; p. JTh2A.75.
28. Vlcak, P.; Sepitka, J.; Drahokoupil, J.; Horazdovsky, T.; Tolde, Z. Structural Characterization and Mechanical Properties of a Titanium Nitride-Based Nanolayer Prepared by Nitrogen Ion Implantation on a Titanium Alloy. *J. Nanomater.* **2016**, *2016*, 9214204. [CrossRef]
29. Gaur, S.; Raman RK, S.; Khanna, A.S. In Vitro, investigation of biodegradable polymeric coating for corrosion resistance of Mg-6Zn-Ca alloy in simulated body fluid. *Mater. Sci. Eng. C* **2014**, *42*, 91–101. [CrossRef]
30. Huang, C.H.; Chen, R.S.; Yoshimura, M. Direct bioactive ceramics coating via reactive Growing Integration Layer method on α-Ti-alloy. *Mater. Sci. Eng. C* **2017**, *76*, 1216–1223. [CrossRef]